

PITCH CONTROL FOR LVRT IMPROVEMENT OF WIND FARM UNDER THE DIFFERENT SHORT CIRCUIT CAPACITY AND REACTIVE POWER SOURCE LOCATION

Aung Ko Thet, Hiroumi Saitoh, Junichi Toyoda
 Graduate School of Engineering, Tohoku University
 Sendai, Japan
 epsys02@ec.ecei.tohoku.ac.jp, saitoh@ecei.tohoku.ac.jp

Abstract – This paper presents a new pitch control to improve the low-voltage ride-through (LVRT) capability of induction-generator-typed wind turbine generators (WTGs). On fault occurrence in the sub-transmission network, the proposed pitch control initiates the WTGs to achieve the fast power reduction. In this way, the over speed and over current of WTGs can be avoided. As the result, the WTGs can continue the connection to the network. In this paper, the effects of grid stiffness and static var compensator (SVC) location on the proposed pitch control are also studied by using the simulation model developed in MATLAB/Simulink with SimPowerSystems Toolbox. The simulation results show that the proposed pitch control system is effective under the different SVC location with different grid stiffness, and the performance of the pitch control system can be also improved by choosing the appropriate gain value according to the response time of pitch control.

Keywords: *Wind power generation, pitch control, low-voltage ride-through, protective relay*

1 INTRODUCTION

To maintain the stability of modern power systems, low-voltage ride-through (LVRT) of a large number of WTGs must be satisfied [1]. This can be achieved by improving the voltage recovery of WTGs with reactive power compensation, adjustment to relay settings of WTGs, and enhancement of WTGs' control ability [2]. Among the WTG types, fixed-speed wind-turbines (FSWTs) with squirrel-cage induction generator (SCIG) is mainly used due to their attractive characteristics such as brushless and rugged construction, low cost, maintenance free, and operational simplicity. For FSWT, either stall-regulated control or active pitch angle-regulated control can be implemented [3]. In our previous paper [4], a new method of controlling the wind turbine pitch angle was proposed to improve the LVRT capability of

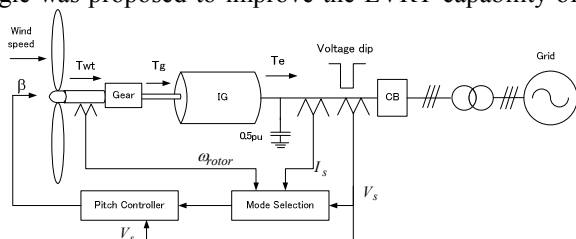


Figure 1: Concept of proposed pitch controller in wind turbine.

wind farm with FSWTs and SVC. The kernel of proposed pitch control is using the fast response under voltage relay to release part of wind power so as to decrease turbine speed and induction generator current during the voltage dip. The releasing power is adjusted by means of the proportional-integral (PI) pitch controller with an input signal of wind turbine terminal voltage.

The aim of this paper is to extend the previous study by taking into account the influence of grid stiffness and SVC location. SCIG in FSWT requires the large reactive power to recover the air gap flux when a short circuit fault occurs in the power systems [5]. Therefore, LVRT behavior of such wind farm can be varied according to the stiffness of grid and location of reactive power source. We particularly study to find the conditions at which the proposed pitch control is effective. This will give the perspective of how to design the pitch control parameters. With this end in view, we evaluate the performance of proposed pitch control by considering the different short circuit capacity (SCC) of power systems at wind farm interconnection point and SVC locations with respect to the different fault points. In addition, the influence on the parameters of controller by the response time of under voltage relay is also evaluated.

The paper is organized as follows. In section 2, the proposed pitch control method is explained. The effectiveness of pitch control for wind farm's LVRT is confirmed by simulation studies. Section 3 describes the simulation models. In Section 4, we perform the simulation and present our simulation results. In section 5, we summarize the paper.

2 PROPOSAL OF PITCH CONTROL FOR LVRT

2.1 Concept of Pitch Control for LVRT

In the FSWT, squirrel-cage induction-generator typed WTGs are implemented. These types of generators absorb reactive power from a power network to supply real power, so that they cannot control their terminal voltage by themselves. This implies that, during the voltage depression caused by a fault occurred in the network, the wind turbine is only able to deliver real power to the network in proportion to the retained voltage. Therefore, as shown in Fig. 1, the power imbalance between mechanical input power, T_{wt} , to the generator and electrical

output, T_e , accelerates the generator rotor. If this situation is allowed to continue, the WTG will reach to over speed limit or over current limit in the wake of the fault and then eventually, the generator will be disconnected by protection systems. So it is vital to balance between the mechanical input power, T_{wt} , and the electrical output, T_e , for enhancing the LVRT capability of FSWT. If the turbine rotor speed can be reduced quickly during voltage dip so as not to rise over the maximum speed, then the sudden disconnection of WTG can be avoided.

The main concept of the proposed pitch angle control is based on the voltage dip detection by fast response of under voltage relay and a feedback PI control of terminal voltage, V_s , during voltage dip. A sudden voltage dip is detected by the under voltage relay to initiate the pitch angle control in LVRT mode. Then, the pitch angle of blades is changed according to the depth of voltage dip so as to suppress the rapid increase of rotor speed by the release of blowing wind power. By this way, the mechanical input power, T_{wt} , can be controlled in order to balance the retarding electrical torque, T_e , of the generator during and after the fault.

2.2 Configuration of Proposed Pitch Controller

The configuration of pitch angle control system consists of three parts: (1) wind turbine protection and pitch angle controller selection, (2) LVRT mode controller, and (3) normal mode controller, as shown in Fig.2. In the first part, the protection relays for the rotor over speed and induction generator over current protection are included. The protection system detects the rotor speed, ω_{rotor} , and generator current, I_s , whether in LVRT pitch control mode or normal mode. If the protection system detects over speeding limit or over current limit [2], wind turbine is disconnected for the safety purpose, and the pitch angle is set to 90° .

The second part is designed to control the pitch angle according to the WTG behavior during voltage dip. The proposed pitch controller for LVRT is illustrated in the part of Fig. 2 enclosed by the dotted lines. The pitch angle β_{LVRT} for LVRT is the output of PI controller which is very widely used for many kinds of control systems. The parameters are presented in section 4.6.

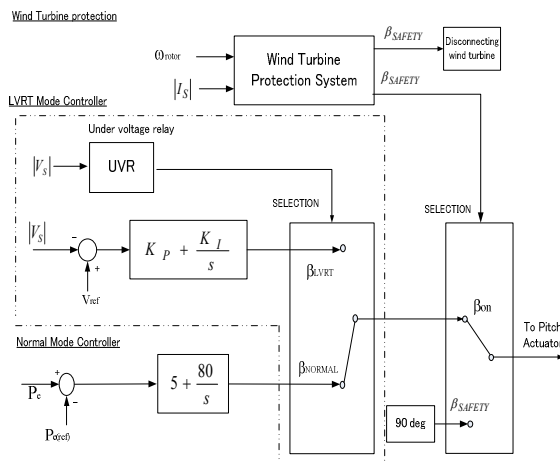


Fig. 2. Block diagram of the proposed pitch control.

The input of the PI controller is the difference between reference voltage, V_{ref} , and the measurement of generator terminal voltage, V_s . When the generator terminal voltage drops below the 0.7 (p.u.) of nominal voltage, the LVRT pitch control mode is activated by the under voltage relay (UVR) with the total delay time of 100ms. It is assumed that this delay time includes the relay pickup time, $T_{pick} < 100ms$ and communication and switching delay. After the monitored voltage, V_s , has recovered for more than 5s, LVRT pitch control mode is deactivated. These under voltage relay time settings used in the study are taken from the reference [6].

The pitch angle control in wind turbine is the most common means of controlling the generated power. Therefore, the pitch controller in normal mode operation is also included as a third part. During the normal mode operation which is determined by the protection system switching logic, the pitch angle is controlled by conventional controller in which generated active power, P_e , is used as an input parameter. When the generated active power is above the rated power, 2MW, the blades are pitched by β_{NORMAL} to reduce the extracted wind power. The explanation of the pitch control mode selection scheme is done in the next section.

2.3 Pitch Control Mode Selection Logic

The pitch control mode selection is done by the coordination of wind turbine protection system. The selection between the two control modes in section 2.2 is based on monitoring the terminal voltage, V_s , the stator current, I_s , of SCIG, and wind turbine rotor speed, ω_{rotor} .

The selection logic for pitch control modes is explained here by using Fig. 3. Firstly, checking of whether the stator current, I_s , or the rotor speed of wind turbine, ω_{rotor} , exceeding the specified limit parameters [2] is carried out. If, at least one of these parameters is exceeded for 40 ms, the safety stop command is sent to pitch controller to set the maximum pitch angle

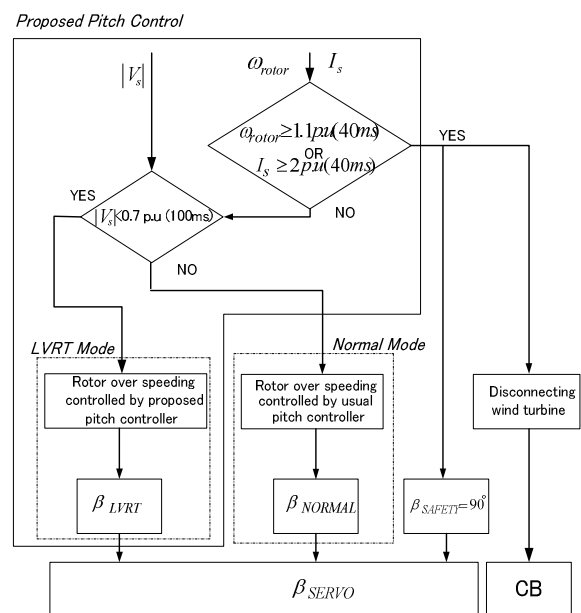


Fig. 3. Flow chart of pitch control mode selection.

($\beta_{\text{SAFETY}}=90^\circ$) and, at the same time, the WTG is disconnected from power network by the operation of circuit breaker (CB). Otherwise, pitch angle, β_{NORMAL} , is set by the normal mode pitch control with the input signal of generated active power unless a voltage dip is detected. If the voltage dip inception is detected, the protection system switches the LVRT mode pitch control action and pitch angle, β_{LVRT} , is set.

3 SIMULATION MODELS

The effectiveness of the proposed pitch control method for LVRT was confirmed by means of simulation studies. The objective of this study is related to the electromechanical dynamic behavior of WTG and hence, only the fundamental frequency component of voltages and currents is taken into account in all the simulation models.

3.1 Power Systems and Wind Farm Model

The power system model including a wind farm shown in Fig.4 is used. The wind farm consists of 15 FSWTs of which each has 2MW rated power capacity [7]. The wind farm is connected to 66kV bus at which SVC of 30 MVar capacity is installed for bus voltage stabilization.

The turbulence nature of wind speed can be neglected because the voltage dip duration is relatively short in LVRT studies. During the normal operation, even the wind blows up to 25 m/s, the maximum possible rotor speed will be around the rated rotor speed. Therefore, it can be considered that the maximum power generation conditions are the worst-cases performance for evaluating LVRT. In this regard, the complicated wind speed model is omitted in the simulation studies, and the rated wind speed of 14m/s is mainly used as the worst-case condition for LVRT.

Moreover, the internal wind farm network and any in-

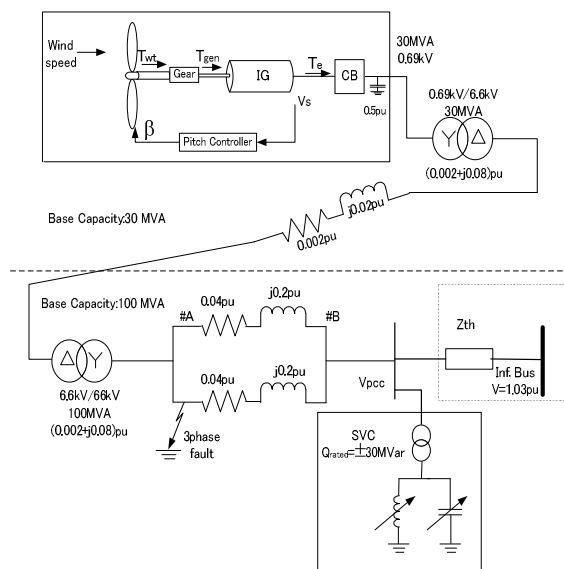


Fig. 4. A model of power systems including wind farm and SVS.

teractions between the turbines themselves are neglected in this study. This implies that, it is not necessary to model individual wind turbines in the wind farm as far as they are in same type and connected to the same bus. Instead, an aggregated wind farm model is used to evaluate the interaction with power systems. The aggregated model is developed by lumping of 15 WTGs into a single equivalent wind turbine. These WTGs are assumed to have the identical system parameters and wind speed on each. The fixed shunt capacitor of (0.5p.u.) [7] is assumed to be connected to each WTG throughout the LVRT.

The power systems is represented by the infinite bus with an equivalent impedance, Z_{th} . The Z_{th} has X/R ratio of 10 and the Z_{th} value is set according to the short circuit capacity (SCC) of power systems, i.e. $(4.356+j43.56)\Omega$ at 100MVA, $(0.8712+j8.712)\Omega$ at 500MVA, and $(0.4356+j4.356)\Omega$ at 1000MVA respectively. The FSWT, CB, wind turbine transformers, SVC, cables and grid transformers [8] are modeled by using the MATLAB/Simulink SimPowerSystems toolbox.

3.2 Static Var Compensator System (SVC) Model

When a wind farm is connected to a power system, the impedance between the wind farm and the system will be dominated by reactance. Therefore, the reactive power flow dominates any voltage variation at the point of wind farm connection. In general, it would be expected that the fast response reactive power compensation device is implemented at the point of wind farm connection to control the voltage variation due to fluctuated nature of wind speed causing the variation in reactive power absorption by SCIG. Therefore, to verify the effectiveness of the proposed pitch control method, it is assumed that a SVC is installed in the power system.

The SVC is modeled as an equivalent current source, I_{SVC} . The current, I_{SVC} , is assumed to be regulated by the control system indicated in Appendix Fig. A1. This model only considers the impact on voltage stability at fundamental frequency [9]. It implies that the details of power electronics, the measurement system, and the synchronization system are represented by simple transfer functions at the system's fundamental frequency. The SVC has the dynamic performance of ± 30 MVar, with the average thyristor valves firing time delay, T_d , of 4ms and the V-I characteristics slope or droop reactance, K_{SL} , of 0.03 p.u. at 30 MVA base. The reference voltage (V_{ref}) of the voltage regulator with PI controller is set at 1.03 p.u. to stabilize the voltage at the Point of Common Coupling (V_{pcc}).

3.3 Induction Generator and Shaft System Model

We use the six order SCIG model to take account the transients in the rotor circuit as well as the fundamental-frequency transients components of stator circuit [7]. All electrical variables and parameters in [7] are referred to the stator.

3.4 Pitch Servo Actuator

A pitch servo actuator model is shown in Appendix 4. In this study, the pitch angle change, $\Delta\beta/\Delta t$, is limited by a possible pitch rate for a modern wind turbine, i.e., $d\beta/dt_{MAX}$ and $d\beta/dt_{MIN}$ at ± 15 [deg/s] respectively [10]. Then the pitch angle is limited between $\beta_{MAX}=90^\circ$ and $\beta_{MIN}=0^\circ$. The servo time constant is set at $T_{SERVO}=0.25s$ [2].

4 SIMULATION RESULTS

The LVRT behavior is evaluated by means of simulation studies. By assuming the different three-phase-to-ground fault points between node #A and #B (at 1km, 8km, 18 km of 19km long sub-transmission line from the node #A respectively) in Fig. 4, the voltage along the sub-transmission lines is depressed until the faulted line is isolated. The fault sequence used in the simulation is the three-phase-to-ground fault occurred in one of the 66kV sub-transmission lines. The fault is occurred at 500 ms and the faulted line is isolated at 700 ms from the start point of simulation. In addition to these, LVRT behaviors of wind farm are explored by considering the two different locations (whether at node #A or node #B) of SVC and the three different stiffness (100MVA, 500MVA, 1000MVA of SCC respectively) of power systems.

4.1 Scenario 1 (SVC at node #B, 500MVA SCC, Fault at 1km from node #A, without pitch control)

The LVRT behavior of wind farm for this scenario is shown in Fig. 5 and 6. The associated SVC behavior is also shown in Fig. 7. In Fig. 5, the generated active power of wind farm is lost at 2098 ms from the start point of simulation due to the wind farm disconnection after isolating the faulted line. When the fault is occurred at the distance of 1km from node #A, the generated terminal voltage is depressed suddenly to 0.5 p.u at the 500 ms. The generator terminal voltage continues depressing to the 0.03 p.u. until the faulted line is isolated at 700 ms. As explained in section 2, the imbalance between mechanical input and electrical output is occurred which causes the rotor over speeding.

Once the faulted line is isolated at 700 ms, the terminal voltage tends to recover back. Consequently, SCIG absorbs more reactive power due to over speeding (not reached to the protection system limit of 1.1 p.u. at that instance) and this causes over current in the stator of SCIG (not reached to the protection system limit of 2 p.u. for 40ms at that instance) as shown in Fig. 5 and Fig. 6. However, the terminal voltage of SCIG is collapsed due to the continuous over speeding of rotor and unfortunately reached to the over speed protective relay limits for 40 ms at the time of 2098 ms from the start point of simulation. Therefore, WTG is disconnected from the grid by over speed protection in order to avoid the damaging.

The behavior of SVC is shown in Fig. 7. Due to the fault, the bus voltage controlled by SVC at node #B is depressed to the 0.5 p.u. until the fault is isolated. Ac-

ording to the reference voltage setting of voltage regulator, SVC injected the reactive power of 30Mvar once the voltage at node #B is recovered back. Although the SVC fed the reactive power absorbed by the wind farm during and after the fault, the continuous power supply of wind farm is cannot be achieved in this case.

4.2 Scenario 2 (SVC at node #B, 500MVA SCC, Fault at 1km from node #A, with pitch control)

The LVRT behavior of wind farm for this scenario is shown in Fig. 8 and 9. The associated SVC behavior is also shown in Fig. 10. With the use of proposed pitch control, the LVRT can be improved. By comparing Fig. 5 with 8, the over speeding of rotor can be reduced during the post-fault period in scenario 2. The rotor speed recovers back to pre-fault level (around 1 p.u.) at 1500ms. Consequently, the proposed pitch control contributes to voltage recovery and reduction of the over current in the stator of SCIG after the fault is isolated as shown in Fig. 8 and 9 respectively.

4.3 Scenario 3 (SVC at node #A, 1000MVA SCC, Fault at 1km from node #A without pitch control)

The LVRT behavior of wind farm in this scenario is shown in Fig. 11 and 12. The associated SVC behavior is also shown in Fig. 13. In Fig. 11, the generated active power of wind farm is lost at 1023 ms from the start point of simulation due to the wind farm disconnection after isolating the faulted line. As shown in Fig. 11, wind farm is disconnected by over current protection.

The behavior of SVC in scenario 3 is shown in Fig 13. Due to the fault, the bus voltage controlled by SVC at node #B is depressed to the around 0 p.u. until the fault is isolated. According to the reference voltage setting of voltage regulator, SVC injected the reactive power of 30Mvar once the voltage at node #B is recovered back. The SVC fed the reactive power absorbed by the wind farm after the fault until the terminal voltage recovers back to the nominal voltage of 1 p.u. Due to the close location to fault, SVC cannot fed reactive power during the voltage dip.

By comparing scenario 1 and 3, the location of SVC with respect to the fault point will affect the reactive power injection during the voltage dip. This will cause the different phenomenon in disconnection of wind farm.

4.4 LVRT Behaviors under different Short Circuit Capacity and Fault Point (SVC at node #B case)

The LVRT behaviors of wind farm are evaluated under different SCC and fault points. Table 1 summarizes the LVRT behaviors of wind farm for these cases in which the SVC is supposed to be connected at the node #B. In this table, the disconnection reason with corresponding time, and fault points are shown according to the SCC. The proposed pitch control is effective for all the cases of 500 MVA SCC and 1000 MVA SCC, as explained in section 4.2. In the 100 MVA SCC case, the proposed pitch control is only effective for the 8 km fault point case. LVRT cannot be achieved for 1 km fault point and 18 km fault point cases. For the 1 km

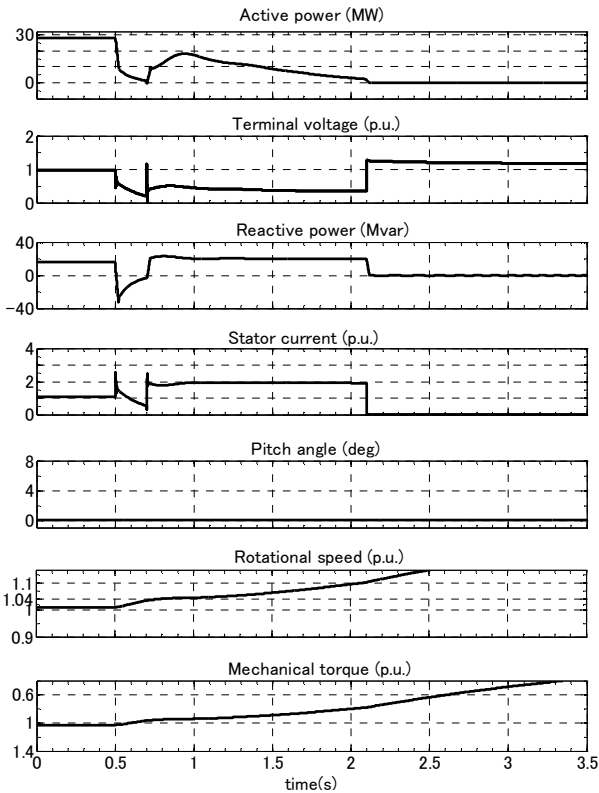


Figure 5: Wind Farm Behavior (Scenario 1: SVC at node #B, 500MVA SCC, fault at 1km from node #A, without pitch control)

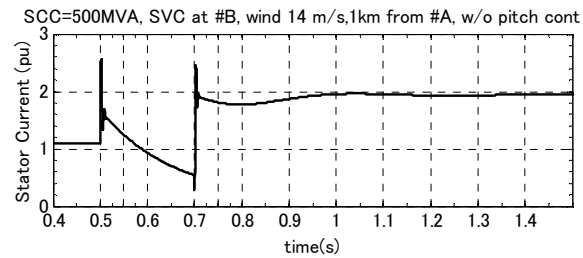


Figure 6: Enlarged plot of stator current in figure 5

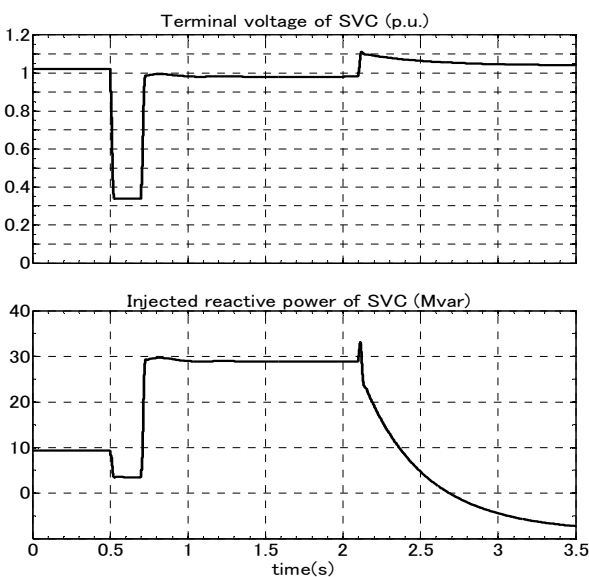


Figure 7: SVC Behavior (Scenario 1: SVC at node #B, 500MVA SCC, fault at 1km from node #A, without pitch control)

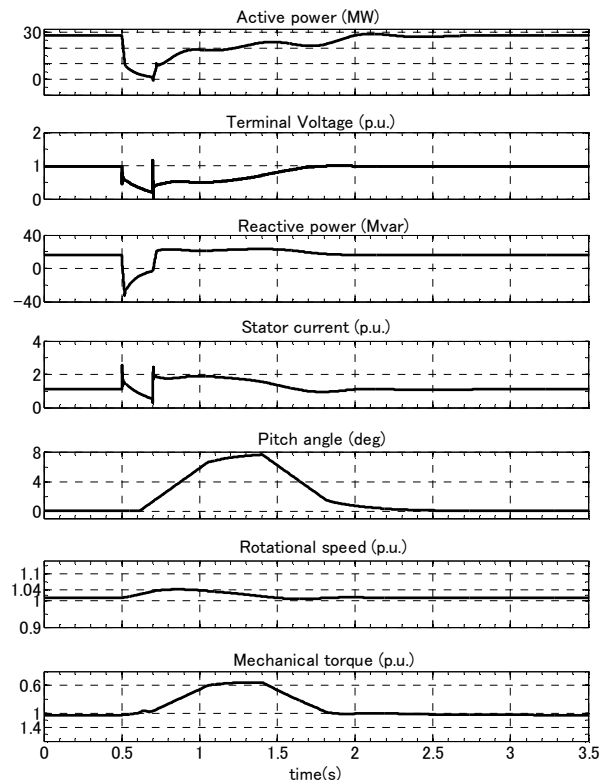


Figure 8: Wind Farm Behavior (Scenario 2: SVC at node #B, 500MVA SCC, fault at 1km from node #A, with pitch control)

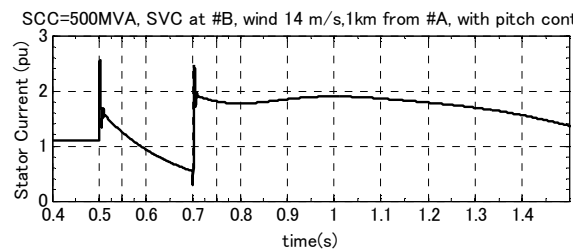


Figure 9: Enlarged plot of stator current in figure 8

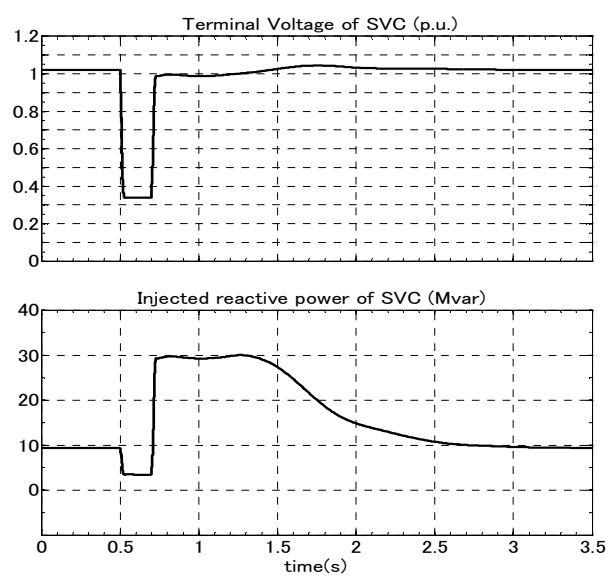


Figure 10: SVC Behavior (Scenario 2: SVC at node #B, 500MVA SCC, fault at 1km from node #A, with pitch control)

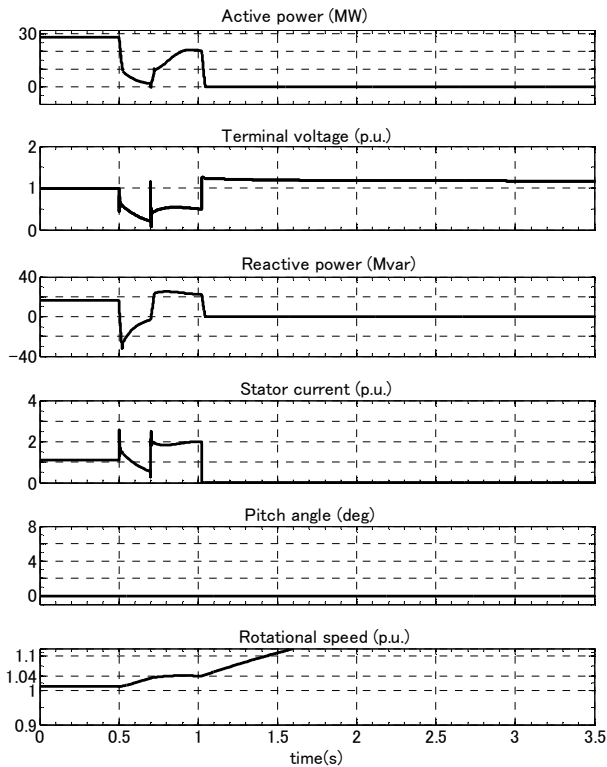


Figure 11. Wind Farm Behavior (scenario3: SVC at node #A, 1000MVA SCC, fault at 1km from node #A, without pitch control)

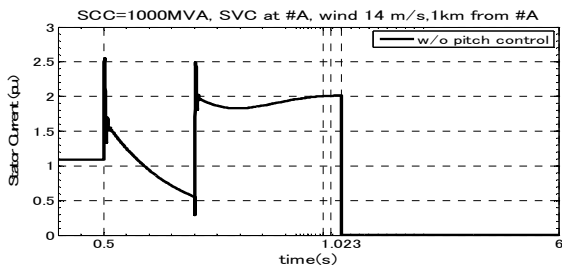


Figure 12. Enlarged plot of stator current in figure 11

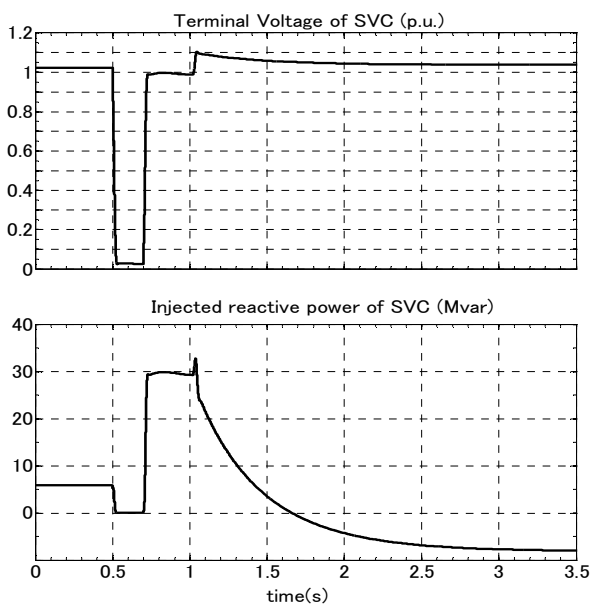


Figure 13. SVC Behavior (scenario3: SVC at node #A, 1000MVA SCC, fault at 1km from node #A, without pitch control)

(SCC)	with pitch control	without pitch control	fault point
100	Over Speed(5.59s)	Over Speed (1.534s)	1km
	Succeed	Over Speed (1.552s)	8km
	Over Speed(5.62s)	Over Speed (1.535s)	18km
500	Succeed	Over Speed (2.098s)	1km
	Succeed	Over Speed (2.392s)	8km
	Succeed	Over Speed (2.131s)	18km
1000	Succeed	Over Speed (2.338s)	1km
	Succeed	Succeed	8km
	Succeed	Over Speed (2.472s)	18km

Table 1. LVRT Behaviors for SVC at node #B

(SCC)	with pitch control	without pitch control	fault point
100	Succeed	Over Speed (1.552s)	1km
	Succeed	Over Speed (1.572s)	8km
	Succeed	Over Speed (1.555s)	18km
500	Succeed	Over Speed (2.315s)	1km
	Succeed	Over Speed (2.998s)	8km
	Succeed	Over Speed (2.382s)	18km
1000	Succeed	Over current (1.023s)	1km
	Succeed	Succeed	8km
	Succeed	Over current (1.071s)	18km

Table 2. LVRT Behaviors for SVC at node #A

fault point case, the voltage recovery capability of WTG is reduced due to the close fault location. Similarly, the fault at 18 km from node #A reduces the voltage support ability of SVC. Therefore, we considered the close location of SVC to the wind farm in evaluation of LVRT in the following section.

The stiffness of power systems influences on LVRT behavior. LVRT can be achieved with the use of only SVC for the 8km fault point in 1000MVA SCC case. This is because the impact of fault on voltage support ability of SVC is less.

4.5 LVRT Behaviors under different Short Circuit Capacity and Fault Point (SVC at node #A case)

Table 2 summarizes the LVRT behaviors of wind farm for the cases in which the SVC is supposed to be connected at the node #A. With the proposed pitch control, the disconnection of wind farm by over speed and over current can be avoided in all conditions.

For the only SVC cases in the 100 MVA SCC and the 500 MVA SCC, as mentioned before, the LVRT cannot be improved as wind farm is disconnected by over speed protection. For 1 km fault point and 18 km fault point cases in 1000MVA, although the continuous connection can be achieved for the 8 km fault point, the wind farm is disconnected by over current protection of WTG. This phenomenon may be related to the close location of reactive power source to the wind farm so as to the voltage variation characteristic of grid.

4.6 Range of controller parameter according to the different SVC location and delay time of UVR

Fig. 14 and Fig. 15 show the relationship between the proportional gain value and UVR relay pickup time

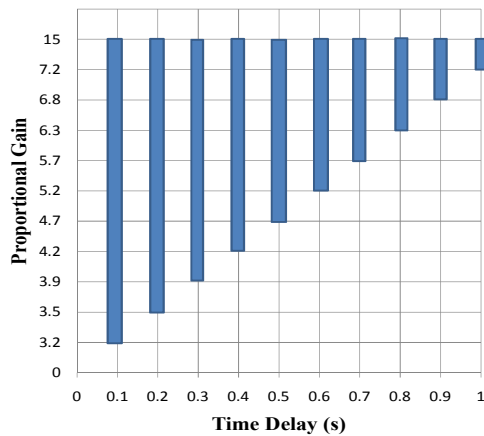


Figure 14: Applicable gain range vs. delay time (SVC at node #A case)

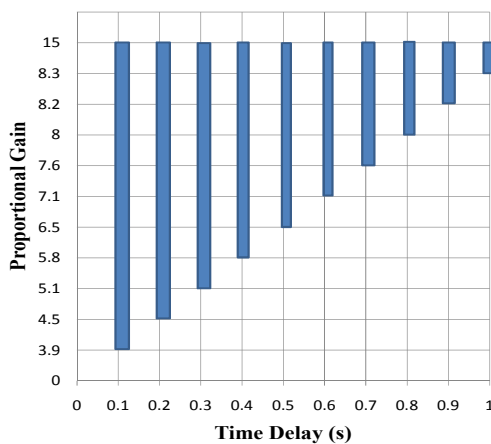


Figure 15: Applicable gain range vs. delay time (SVC at node #B case)

delay in the case of 500 MVA SCC when the SVC is connected at node #A and #B, respectively. For the fastest response time, 0.1s, the LVRT can be achieved with the proportional gain value between 3.2 and 15 in the case of SVC at node #A, and between 3.9 and 15 in case of SVC at node #B. Beyond the gain value of 15, the active power oscillation is observed during the voltage recovery period. The integral gain value can be applied up to 50 with respect to those proportional gains. The trend of narrowing the range of gain value can be found in increasing time delay to initiate the pitch control.

5 CONCLUSION

This paper presents the effects of grid stiffness and static var compensator (SVC) location on the proposed pitch control for LVRT. The use of proposed pitch control is effectiveness in reasonable grid stiffness scenarios. Moreover, the ranges of controller parameters are presented accordingly. Using proposed pitch control only requires small modifications in the control of existing FSWTs. With the expectation of advance technology development in wind turbine parts for less mechanical stress, the proposed pitch control is worthwhile to use as an additional back up counter measure for LVRT.

According to our study, the LVRT behavior is closely related to the voltage recovery after clearing the fault. Therefore, the stiffness of grid and location of reactive power source should be taken into account in LVRT studies. The detail studies to find out the relationship of PI controller parameters to the grid stiffness, time delay in initiating the pitch control are the future works.

6 APPENDIX

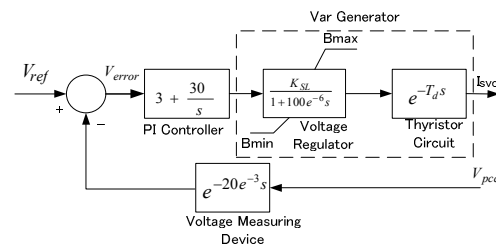


Figure A1: Block diagram of SVC

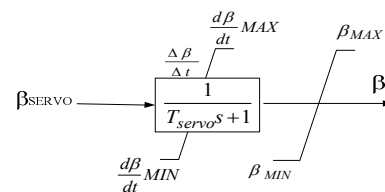


Figure.A2: Pitch actuator model.

Parameters of wind turbine model: [7]

Nominal rotor speed: 17 RPM, Shaft stiffness: 0.3pu/el.rad, Rotor diameter: 75m, Area covered by rotor: 4418m², Nominal power: 2 MW, Nominal wind speed: 14m/s, Gear box ratio: 1:89, Inertia constant: 2.5s,

Coefficients of Approximation in Aerodynamic Power:[7]

C₁=0.73, C₂=151, C₃=0.58, C₄=0.002, C₅=2.14, C₆=13.2, C₇=18.4, C₈=-0.02, C₉=-0.003,

Parameters of induction generator model:[7]

Number of poles: 4, Generator speed: 1500 RPM, Mutual inductance: 3.0p.u, Stator leakage inductance: 0.1p.u, Rotor leakage inductance: 0.08p.u, Stator resistance: 0.01p.u, Rotor resistance: 0.01p.u.

REFERENCES

- [1] M. Tsili S. Papathanassiou, "A review of grid code technical requirements for wind farms", IET Renewable Power Generation, 2009, Vol. 3, pp. 308-332A.
- [2] Vladislav Akhmatov, Induction Generators for Wind Power. Brentwood, U.K.: Multi-Science Publishing, 2007.
- [3] J. F. Manwell, J. G. McGowan, A. L. Rogers, Wind energy explained: theory, design and application Chichester, U.K.: Wiley, 2009, 2nd edn, pp.371-373.
- [4] A. Ko Thet and H. Saitoh, "Pitch Control for Improving the Low-Voltage Ride-Through of Wind Farm." Proceedings of IEEE T&D Asia - SIEF 2009, OR3-7, 2009.
- [5] Claudio L.Souza et. Al., "Power System Transient Stability Analysis Including Synchronous and Induc-

- tion Generator,” IEEE Porto Power Tech Proceeding, Vol. 2, pp.6, 2001.
- [6] <http://www.benderrelay.com/voltage%20relays%20table.htm>, SUR 353Z-71, 3 AC 690V, 0.7-0.95 Un, 50-60 Hz, download on 2008-July-1.
- [7] J.G. Slootweg, H. Polinder, W.L. Kling, Representing Wind Turbine Electrical Generating Systems in Fundamental Frequency Simulations. IEEE Transactions on energy conversion, vol: 18, No.4, December 2003.
- [8] R. Takhashi, J. Tamura, Y. Tomaki, A. Sakahara, E. Sasano, Wind Farm Stabilization by Variable Speed Wind Energy Conversion System using Permanent Magnet Synchronous Generator. IEEJ, RM-05-114 (in Japanese).
- [9] MATLAB R2009a, Manual, MathWorks, Inc., 2009.
- [10] S. Heier, Grid Integration of Wind Energy Conversion Systems. Chichester, U.K.: Wiley, 2006, 2nd edn.